PERGAMON

Journal of Structural Geology 23 (2001) 803–806

JOURNAL OF STRUCTURAL GEOLOGY

www.elsevier.nl/locate/jstrugeo

Quantitative estimation of exponents of power-law flow with confidence intervals in ductile shear zones

Kieran F. Mulchrone*

Department of Applied Mathematics, National University of Ireland, Cork, Republic of Ireland

Received 19 November 1999; accepted 12 October 2000

Abstract

Talbot (Journal of Structural Geology 21, 1535–1551, 1999b) introduced a new model for ductile shear zones as counterflow boundaries in pseudoplastic power-law fluids, and demonstrated that natural shear zones empirically fit theoretical curves generated by his model. Thus estimates of the power-law exponent relating stress and strain are deduced. It is shown here how application of standard non-linear statistical techniques to shear zone displacement data allows quantitative estimation of the power-law exponent together with confidence intervals of the calculated value. Application to natural shear zones verifies the method and also validates the applicability of the model. It is hoped that this will encourage field geologists to apply the model of Talbot to natural examples. Thereby a database of power-law exponents for a wide variety of lithologies and metamorphic grades may be assembled.

1. Introduction

The primary objective of this paper is to enhance and simplify the practical application of the ductile shear zone model of Talbot (1999b) by introducing quantitative methods for calculating the power-law exponent. The model of Talbot (1999b) considers ductile shears as counterflow boundaries in pseudoplastic fluids. It is not the purpose of this paper to review or enhance the model and the interested reader is referred to the original paper for more detail.

Talbot (1999b) estimated the power-law exponent for natural shear zones by visually comparing suitably scaled theoretical curves to photographs. Though this method is valid, it is also subjective and requires a certain degree of effort and trial and error, which may dissuade some from applying the model. A relatively simple quantitative method is presented below for estimating the power-law exponent together with confidence intervals for the calculated value.

It is hoped that this contribution removes a potential obstacle to the widespread application of the model and that field data can be more rapidly and easily converted into power-law exponent values. Thus a database of power-law exponents from various lithologies deformed during different PT conditions can be assembled. Such a database may allow important conclusions regarding the behaviour of rocks to be drawn and together with viscosity data may enable definition of quantitative deformation facies (Talbot, 1999a).

2. Development of the method

2.1. Non-linear parameter estimation

Talbot (1999b) has proposed that the relationship between displacement (u) parallel to a half shear zone (HSZ) and the normal distance from the boundary of a HSZ (y) is as follows:

$$\frac{u}{u_{\max}} = 1 - \left(\frac{y}{w}\right)^{n+1} \tag{1}$$

where $u_{\max}$ represents the total displacement across the HSZ and w is the total width of the HSZ and n is the power-law exponent (see Fig. 1). Eq. (1) may be linearised by taking natural logarithms of both sides, which after rearrangement is given by

$$\ln\left(1 - \frac{u}{u_{\max}}\right) = (n+1)\ln\left(\frac{y}{w}\right). \tag{2}$$

However, statistical simulations of estimation of n using Eq. (2) and standard linear least-squares regression indicates that Eq. (2) violates fundamental assumptions of linear regression and will not always give reliable results.

Non-linear methods for parameter estimation are therefore applied and developed for Eq. (1). For the sake of

* Tel.: +353-21-902-378; fax: +353-21-270-813.
E-mail address: k.mulchrone@ucc.ie (K.F. Mulchrone).

0191-8141/01/$ - see front matter
PII: S0191-8141(00)00151-6

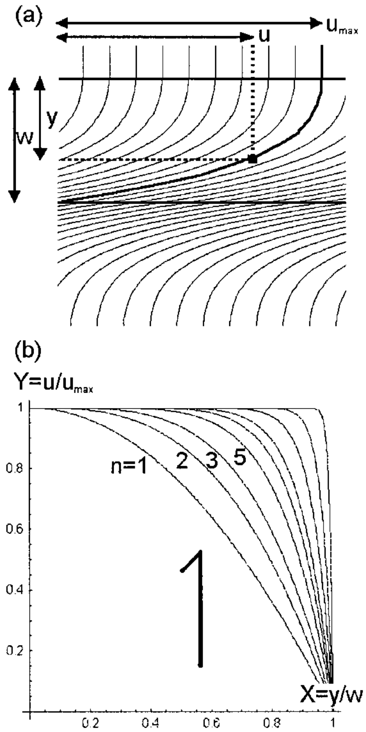

Fig. 1. (a) Schematic illustration of an ideal dextral shear zone with u, u_{max}, y and w identified for the upper half. (b) A plot of the function $Y = 1 - X^{n+1}$ for several values of n. Shear sense is indicated to enable visualisation of how these curves relate to shear zones in the field.

simplicity let

$$Y = \frac{u}{u_{max}} \qquad \text{and} \qquad X = \frac{y}{w} \tag{3}$$

and our model equation becomes

$$Y = f(X,\ n) = 1 - X^{n+1}. \tag{4}$$

Standard non-linear parameter estimation (Draper and Smith, 1981) involves a first-order Taylor series approximation giving

$$Y = f(X,\ n_{e-1}) + \left.\frac{\partial f}{\partial n}\right|_{n=n_{e-1}} (n_e - n_{e-1}) \tag{5}$$

$$Y = 1 - X^{n_{e-1}+1} - X^{n_{e-1}+1}\ln(X)(n_e - n_{e-1}) \tag{6}$$

where n_{e-1} is a previous estimate for n (initially this may be a guess) and n_e is a better estimate for n. Eq. (6) is linear in $X^{n_{e-1}+1}$ and $X^{n_{e-1}+1}\ln(X)$ and is readily compared to the linear equation

$$Y = a + bX_1 + cX_2 \tag{7}$$

where

$$a = 1 \tag{8}$$

$$b = -1 \tag{9}$$

$$c = -(n_e - n_{e-1}) \tag{10}$$

$$X_1 = X^{n_{e-1}+1} \tag{11}$$

$$X_2 = X^{n_{e-1}+1}\ln(X). \tag{12}$$

By taking a set of m data points $(Y_i,\ X_{1i},\ X_{2i})$ where $i = 1$ to m, standard multiple linear regression is applied to estimate n_e. The estimate for c in Eq. (7) is given by

$$c = \Big[\sum Y_iX_{2i}\Big(\sum X_{1i}\Big)^2 - \Big(\sum X_{1i}X_{2i}\sum Y_i + \sum X_{2i}\sum Y_iX_{1i}\Big) \times \sum X_{1i} + \sum X_{1i}^2\sum X_{2i}\sum Y_i + m\Big(\sum X_{1i}X_{2i}\sum Y_iX_{1i} - \sum X_{1i}^2\sum Y_iX_{2i}\Big)\Big] \Big/ \Big[\sum X_{2i}^2\Big(\sum X_{1i}\Big)^2 - 2\sum X_{1i}X_{2i}\sum X_{2i} \times \sum X_{1i} + \sum X_{1i}^2\Big(\sum X_{2i}\Big)^2 + m\Big(\Big(\sum X_{1i}X_{2i}\Big)^2 - \sum X_{1i}^2\sum X_{2i}^2\Big)\Big]. \tag{13}$$

From Eq. (10) the following iterative relationship for n_e is

Table 1
Results of application to natural shear zones

Example	Source	n	Confidence interval	Estimate from Talbot (1999b)
1	Talbot (1999b) fig. 9(c). An older foliation distorted in gneisses at Cristallina, Swiss Alps (originally from Ramsay and Huber, 1983, fig. 3.18)	5.285	0.0002	5
2	Talbot (1999b) fig. 9(c). As example 1	5.468	0.0002	5
3	Talbot (1999b) fig. 9(d). HSZ in Archean migmatites near Holsteinborg, W. Greenland	3.905	0.0009	5
4	Talbot (1999b) fig. 11(d). The Alpine fault, New Zealand (originally from Weijermars, 1987, fig. 10)	2.774	0.0005	3
5	HSZ from Roan, Nord Trøndelag, west central Norway, in amphibolite facies metasediments	2.51	0.05	N/A
6	As example 5	5.7	0.05	N/A
7	Dilational shear zone with an en échelon vein array in bedded sandstones, Barley Cove, West Cork, Ireland, see Fig. 2	1.11	0.01	N/A
8	As example 7	1.35	0.05	N/A

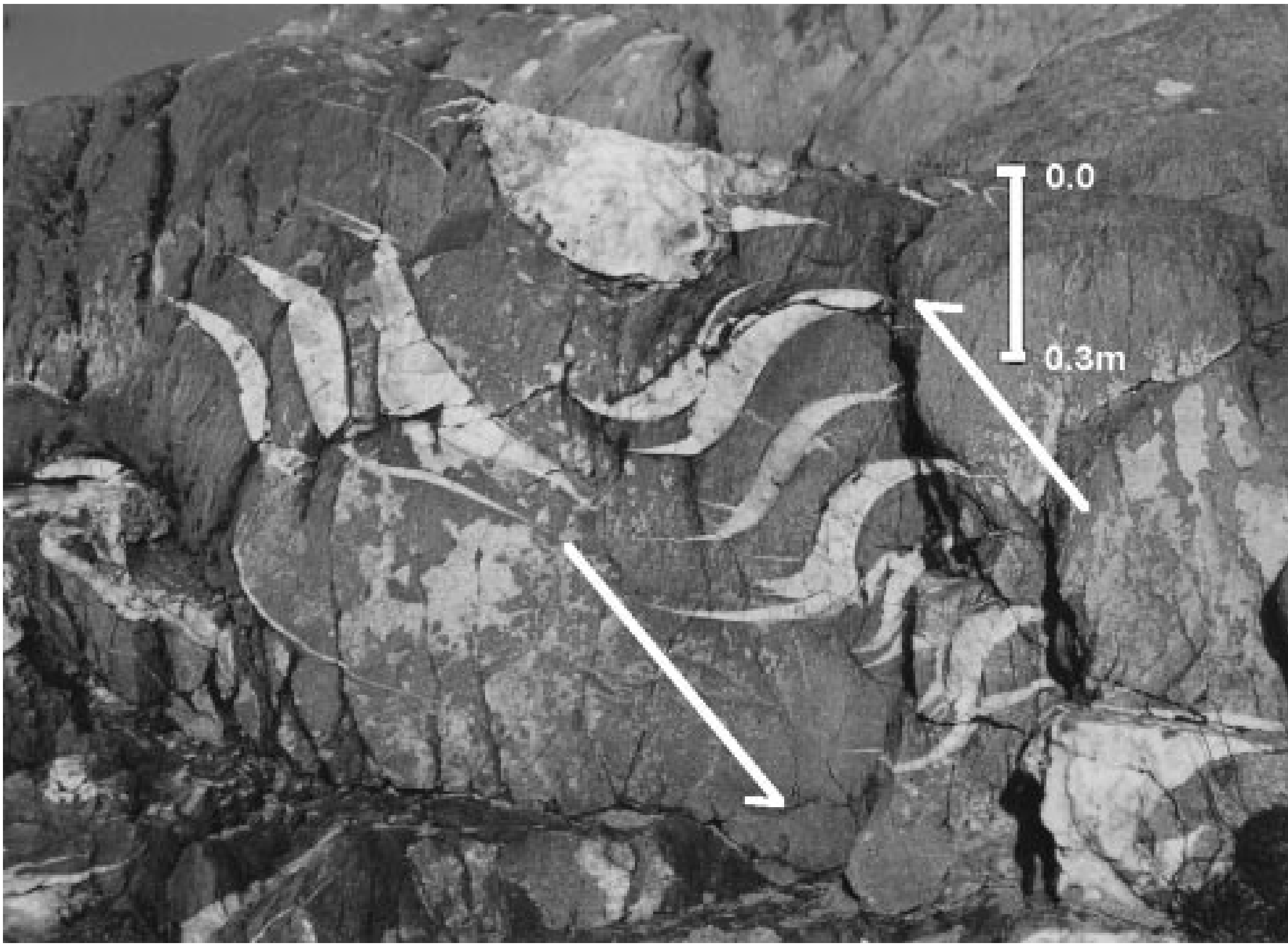

Fig. 2. Dilational shear zone in bedded sandstone, Barley Cove, West Cork, Ireland. Thickened, sigmoidal veins in en échelon, indicate dilation.

derived

$$n_e = n_{e-1} - c \tag{14}$$

Note that each time Eq. (14) is iterated a new value for c must also be calculated. The computed estimate (denoted by $\hat{n}$) is equal to n_e such that

$$|n_e - n_{e-1}| < \delta \tag{15}$$

where δ is a small value. The smaller the value of δ the more accurate the solution becomes.

2.2. Error estimation

Although it may be possible to analytically derive a simple expression for the error associated with $\hat{n}$, it is felt that the easiest approach for the current problem is to apply the bootstrap method (Efron, 1979). Given a set of m measurements for (X_i, Y_i) the estimate $\hat{n}$ is calculated as described above. Typically application of the bootstrap method involves generating another set of m measurements (X_i^*, Y_i^*) by resampling the original dataset with replacement. Another estimate $\hat{n}^*$ may be calculated for (X_i^*, Y_i^*). Resampling may be performed an arbitrary number of times such that a distribution of the estimate $\hat{n}^*$ is derived and is referred to as the bootstrap distribution. The bootstrap distribution of $\hat{n}^*$ tends to coincide with the actual (but unknown) distribution of $\hat{n}$. Hence the standard deviation of the distribution of $\hat{n}^*$ gives an estimate for the standard deviation of $\hat{n}$.

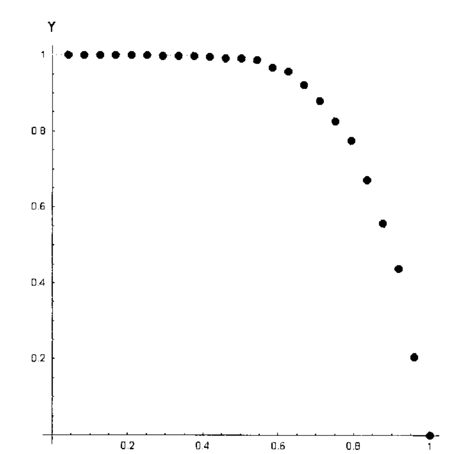

Fig. 3. (X, Y) data for example 1, together with fitted theoretical curve for $n = 5.285$.

In the current problem however, it is likely that datasets will be quite small probably of the order of 20 measurements or so. This is a potential problem for the bootstrap technique described above. However, the following approach, similar to the bootstrap method, is optimal. Given a set of m measurements for $(X_i,\ Y_i)$ and an estimate $\hat{n}$, the residuals (r_i) are calculated as follows:

$$r_i = Y_i - (1 - X_i^{\hat{n}+1}). \qquad (16)$$

The standard deviation (s) of r_i is calculated. Resampled datasets are generated as follows:

$$(X_i^*,\ Y_i^*) = (X_i,\ Y_i + sN(0,\ 1)) \qquad (17)$$

where $N(0, 1)$ is a randomly generated number from the standard normal distribution. Thus by generating arbitrarily many such datasets the error associated with $\hat{n}$ is estimated from the distribution of $\hat{n}^*$.

3. Application to natural shear zones

In this section the quantitative method for calculating the power-law exponent is applied to four HSZs presented in Talbot (1999b) and also for other HSZs observed by the author. The method was not applied to all HSZs presented in Talbot (1999b) because some photographs are too small to allow accurate measurement.

Prior to applying the method, it is instructive to consider Eq. (4) graphically in Fig. 1(b). Fig. 2 of Talbot (1999b) presents a similar graph but, because these theoretical curves are used for visual fitting, $u/u_{\max}$ is plotted on the ordinate axis and y/w on the co-ordinate axis. Traditionally Eq. (4) is plotted as shown in Fig. 1(b) and it is felt that this plot, together with Fig. 1(a), clarifies how one should take measurements in the field or from photographs. y is measured from the HSZ outer margin (i.e. low strain portion), with increasing y-values occurring towards the high strain inner margin. In contrast u is measured with increasing values in the direction of shear.

A computer program has been written to do the calculation and is available as an electronic annex to this paper. The program runs on Windows and allows data entry, saving to file and will calculate $\hat{n}$ and the associated error. It is important that measurements are taken according to Fig. 1(a) and that both u and y vary from zero to their respective maximums. By noting that the method presented above involves the natural logarithm of X, the value of y cannot be zero. This means that one data point is usually omitted from the analysis.

The results of applying the method to eight HSZs are displayed in Table 1. The results are in strong agreement with those of Talbot (1999b). However, differences in values are probably related to the increased precision facilitated by the quantitative method. The data from natural HSZs are well modelled by Eq. (4) and fitted curves are almost exact (see Fig. 3), which lends support to the applicability of Talbot's model to ductile shear zones. If the model were grossly incorrect one would expect a consistent deviation from the model of Eq. (4).

Examples 1, 2, 3, 5 and 6 come from high-grade gneisses and metasediments and give values for $n > 2.5$. In contrast examples 7 and 8 come from relatively low-grade sedimentary rocks and n is close to 1 in value. Although, it is tempting to suggest that higher grade rocks behave as pseudoplastic power-law fluids with $n > 2.5$, whereas low-grade rocks behave almost like Newtonian fluids ($n = 1$), the data are too few. In addition, examples 7 and 8 are from a dilational shear zone and dilation may affect the value of n (Fig. 2). Much more data are required before any hypothesis can be formulated.

4. Conclusions

It is shown how to quantitatively apply Talbot's model to natural shear zones using non-linear parameter estimation.

Values for the power-law exponent and corresponding confidence intervals were calculated for natural shear zones. The results verify values calculated by visual methods in Talbot (1999b) and also validate that natural shear zones are accurately described by the model.

Acknowledgements

I thank Ms Kathleen O'Sullivan, Director, Statistical Laboratory, UCC, Professor Christopher Talbot, Hans Ramberg Tectonic Laboratory, Uppsala, Sweden and Professor Finbarr O'Sullivan, Dept. Statistics, UCC, for reviewing the contents of this paper and for making some helpful suggestions. This paper benefited greatly from the constructive reviews of Drs David Waltham, Graham Yielding and Richard J. Lisle.

References

Draper, N.R., Smith, H., 1981. Applied Regression Analysis. Wiley, New York.

Efron, B., 1979. The Bootstrap, the Jacknife and other Resampling Plans, CBMS-NSF Regional Conference Series. SIAM, PA.

Ramsay, J.G., Huber, M.I., 1983. The Techniques of Modern Structural Geology: Volume 1: Strain Analysis. Academic Press, London.

Talbot, C.J., 1999a. Can field data constrain rock viscosities? Journal of Structural Geology 21, 949–957.

Talbot, C.J., 1999b. Ductile shear zones as counterflow boundaries in pseudoplastic fluids. Journal of Structural Geology 21, 1535–1551.

Weijermars, R., 1987. The construction of shear strain profiles across brittle–ductile shears. Annales Geophysicae 5B, 201–210.